

# Comparative Assessment of PID Controller Tuning Methods for Coffee Roasting Process

Mohamad Taib Miskon<sup>1</sup>, \*Mohd Hezri Fazalul Rahiman<sup>1</sup>, Mohd Nasir Taib<sup>1,2</sup>, Ramli Adnan<sup>1</sup>

<sup>1</sup>Faculty of Electrical Engineering, Universiti Teknologi MARA, Shah Alam, Selangor, Malaysia

<sup>2</sup>Malaysia Institute of Transport (MITRANS), Universiti Teknologi MARA, Shah Alam, Selangor, Malaysia

Corresponding author\* Email: hezrif@uitm.edu.my

Accepted 1 November 2021, available online December 2021

## ABSTRACT

Time-temperature progression of a batch of coffee beans during roasting has been one of the most critical parameters. The roast operator uses it to replicate particular flavour profiles that come to their mind. Therefore the replication of the temperature progression is done mainly using a widely available PID controller. However, the controller is rarely optimized to its best performance due to the difficulty of the PID parameter tuning. This paper presents a comparative performance evaluation of PID controller design using different tuning methods, including Ziegler-Nichols, Cohen-Coon and approximate M-constrained Integral Gain Optimization (AMIGO). The evaluation includes step responses, set-point tracking and disturbance rejection aspects of the controller. The performance indices used in this work incorporate rise time, per cent overshoot, settling time, and integral indices, including ISE, IAE and ITEA. Simulation results indicated that PID-AMIGO had been the best performing controller in all performance assessments except for slow varying set point tracking. The PID-CC controller offered better performance than the PID-AMIGO controller with a 99.8% and 92.5% improvement of the ISE and IAE index, respectively, subject to ramp input.

**Keywords:** Coffee Roasting, Temperature Regulation, PID Tuning

## 1. Introduction

Roasting process has been considered the most crucial step in coffee processing as nearly all of the coffee taste will be developed based on how the beans are roasted [1][2]. It helps develop the coffee flavour from thousands of chemical reactions within the bean during roasting [3]. An amount of heat is applied to a pile of coffee beans during roasting based on a specific time-temperature profile that the roastmaster determined to reproduce the desired taste profile. Since coffee is roasted in batches, in order to ensure the same quality of roasted coffee is achieved in every batch, precise control is essential. The controller's objective would be to follow a specific time-temperature profile and to stabilize the temperature should there be any heat disturbance during the process. This can be achieved using a number of control strategies

Most of the existing commercial coffee roasting machine today employs a conventional Proportional-Integral-Derivative (PID) controller to control the temperature progression of the batch of the coffee bean within the roasting chamber. However, real-time PID controllers are rarely tuned to their optimum setting due to operator incompetence, tuning difficulty and time constraints [4]. It is highly dependent on the operator's knowledge about the dynamic of the process and might cause a problem if the operator retires. The tuning process can be done in frequency response or time response to achieve the desired control performance. Throughout the literature, many tuning techniques have been proposed based on the desired performance criterion. Among the popular tuning method includes the Ziegler-Nichols method, Cohen and Coon method, and approximate M-constrained integral gain optimization (AMIGO) [5][6][7][8].

In this paper, a comparison of controller performance to regulate the temperature of a pile of coffee beans under roasting was evaluated based on different PID tuning approaches. The main objectives are to obtain the lowest overshoot percentage, least settling time and a good disturbance rejection feature.

The organization of this paper is as follows: Section II describes the small-scale coffee roasting process plant and the first-order model used in this study. Section III describes the PID structure and tuning methods used in this study. Section IV details out the comparison of results obtained from the simulation, including set-point regulation and disturbance rejection. Lastly, Section V will describe the conclusion of the study.

## 2. Methodology

### 2.1 Process Model

In this study, the roasting process was carried out using a small-scale coffee roasting plant based on Fresh Roast SR500 air roaster manufactured by Home Roasting Supplies, USA, as shown in Figure 1. Across the literature, this type of roaster can also be seen being used by other researchers for crack sound prediction [9], roast degree determination [10] and also the development of chemical composition under different roast conditions [11]. In this work, an additional K-type thermocouple probe was added inside the roasting chamber to measure the bean pile temperature during roasting. In addition, the control board was also upgraded to enable real-time data collection and control via MATLAB software. The detailed specification and modifications of the SR500 roaster have been described in previous work [12].

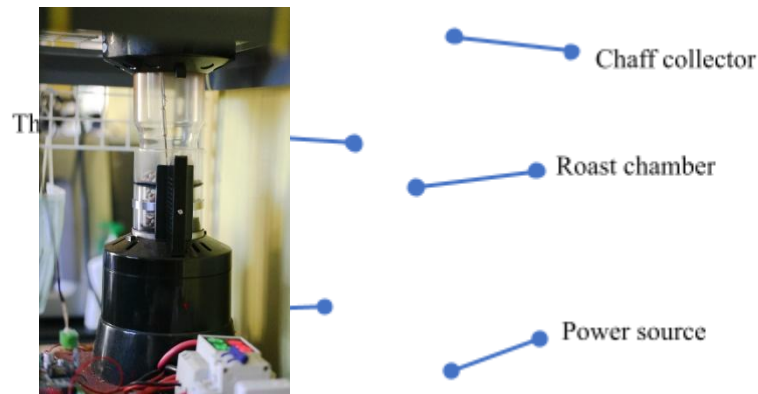


Figure 1. Coffee roasting plant based on Fresh Roast SR500

A linear model based on First Order Plus Dead Time (FOPDT) was estimated using open-loop temperature response data from the roasting process shown in Figure 2(a). The heater level was initially set at 0%, and the bean pile temperature was measured at room temperature, which was 32°C. After 65 s, the heater level was stepped from 0% to 50% to achieve a new steady-state temperature value to allow the drying stage of the coffee bean. At this stage, the colour of the coffee bean will change from green to yellow. Next, a second step change was introduced from 50% to 100% heater level to move the process temperature to a new steady-state value that will indicate the maximum temperature that SR500 can produce at 100% heater level. The temperature response indicated that the process gain is almost identical for both step changes, where the ratio between the changes of the heater step and the corresponding temperature output magnitude is about 1:2. Therefore, it was a good indication of the linear nature of the process [13]. Thus, within the operating temperature between 32°C to 230°C, the process can be approximated using the FOPDT structure given by:

$$G_p(s) = \left( \frac{K}{\tau s + 1} e^{-\theta s} \right) \quad (1)$$

where  $K$  represents the process gain,  $\tau$  indicate the process time constant and  $\theta$  is the dead time. Process gain,  $K$  can be calculated by dividing the steady-state change in the process variable with the step input that contributed to that change [13]. Meanwhile, the time constant  $\tau$  is estimated using the time interval starting from the temperature shows a clear initial response to the step change to the time when the temperature reaches 63.2% from its new steady-state value.

Next, the dead time,  $\theta$  can be obtained by measuring the period when the output temperature started to provide a clear initial response from the time the step change was introduced. Thus based on Figure 2(b), the FOPDT model parameters can be identified as :

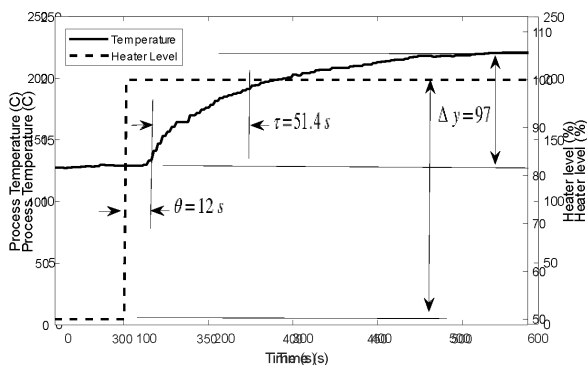
$$K = 1.8, \tau = 51.4s, \theta = 12s$$

Next, these parameters were adjusted to best match the actual data. The matching process was carried out based on the heuristic method, and the discrepancy between the generated model with the actual data was evaluated using the root mean squared error (RMSE) index as tabulated in Table I. A small RMSE value will indicate a better accuracy of the model to represent the roasting process within the observed temperature range. Figure 2(c) depicts the comparison between the actual temperature data and the data generated from the FOPDT model. Thus, the FOPDT model that will be used in this work is given by:

$$G_p(s) = \left( \frac{1.9}{45s + 1} e^{-10s} \right) \tag{2}$$

Table 1. FOPDT model parameters tuning

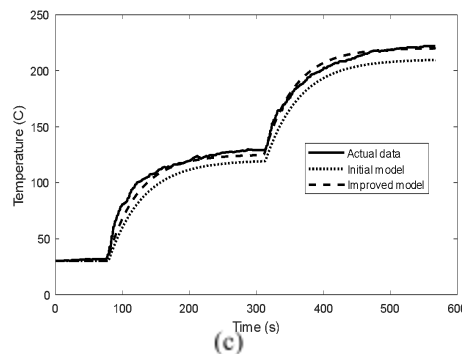
$K$	$\tau$	$\theta$	RMSE	Remarks
1.8	51.4	12 s	10.35	Initial model
1.9	45	12	7.20	Improved model
<b>1.9</b>	<b>45</b>	<b>10</b>	<b>4.11</b>	
2.0	45	12	8.06	



(a)

$\Delta u = 50$

(b)



(c)

Figure 2. (a) Temperature response from an open-loop test at different heater levels, (b) estimation of FOPDT model parameter based on transient response. (c) comparison between the generated model with the actual temperature data.

2.2 PID Structure

PID controller structure can be expressed in the time domain as shown in equation (3), where the output of the controller is represented as  $u(t)$ , while  $e(t)$  is the error signal,  $K_c$  represents the proportional gain,  $\tau_i$  is the integral time and  $\tau_d$  is the derivative time.

$$u(t) = K_c \left( e(t) + \frac{1}{\tau_i} \int e(t) dt + \tau_d \frac{de}{dt} \right) \tag{3}$$

By taking the Laplace transform of equation (4), the transfer function of the PID controller is expressed as

$$C(s) = K_c \left( 1 + \frac{1}{\tau_i s} + \tau_d s \right) \tag{4}$$

However, the pure derivative term  $\tau_d s$  can cause abrupt change to the set-point and may lead to inappropriate manipulated variable values. Thus, to overcome this, a derivative filter is introduced and added to the derivative term as

$$\frac{\tau_d s}{N s + 1} \tag{5}$$

where  $N$  usually is being set somewhere between 2 and 20 [14]. A large  $N$  value will bring PID controller closer to its original form shown in equation (4), and if the  $N$  is approaching 0, the PID controller will collapse to a standard PI controller as the derivative term becoming zero [5]. The simulation of the controller was carried out using MATLAB-SIMULINK, as shown in Figure 3.

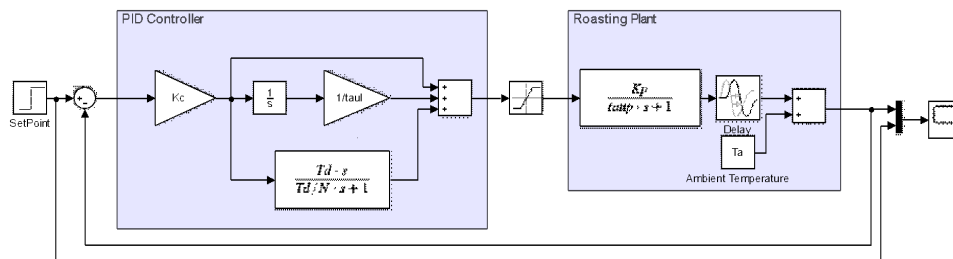


Figure 3. Realization of the PID controller using MATLAB-SIMULINK

The PID controller must be designed to achieve stable operation in both transient and steady-state conditions. Thus, it is essential to tune the controller to get the optimal values of  $K_c$ ,  $\tau_i$  and  $\tau_d$  to achieve the desired performance parameter, such as system overshoot, rise time, and settling time. There are several types of tuning procedures available in control literature. In this paper, the PID tuning method used based on Ziegler-Nichols, Cohen Coon, and AMIGO are summarized in Table 2

Table 2. PID tuning parameters as a function of  $K$ ,  $\theta$ ,  $\tau$  derived from the FOPDT model [5]

Tuning Method	$K_c$	$\tau_i$	$\tau_d$
Ziegler-Nichols	$\frac{1.2\tau}{K\theta}$	$2\theta$	$0.5\theta$
Cohen Coon	$\frac{1}{K} \frac{\tau}{\theta} \left( \frac{4}{3} + \frac{\theta}{4\tau} \right)$	$\theta \frac{32 + 6\theta/\tau}{13 + 8\theta/\tau}$	$\theta \frac{4}{11 + 2\theta/\tau}$

$$\text{AMIGO} \quad \frac{1}{K} \left( 0.2 + 0.45 \frac{\tau}{\theta} \right) \quad \frac{0.4\theta + 0.8\tau}{\theta + 0.1\tau} \theta \quad \frac{0.5\theta\tau}{0.3\theta + \tau}$$

In this paper, three PID controllers were developed based on their corresponding tuning rule. PID-ZN will represent the PID controller tuned by the Ziegler-Nichols method, PID-CC controller used Cohen-Coon tuning method, and PID-AMIGO employed AMIGO tuning rule as its tuning method. Meanwhile, the N parameter for the derivative filter in equation (5) was selected based on each controller's smallest Integral Absolute Error (IAE) index, as shown in table 3. This was done by feeding each controller with step input, and the IAE value was measured for N=2, N=10 and N=20. Based on the findings, N = 2 will be considered for PID-AMIGO, and N= 10 will be used for both PID-ZN and PID-CC controllers.

**Table 3.** Filter setting for PID controller based on IAE

Controller	N	IAE ( $\times 10^2$ )
PID-AMIGO	N=2	5.59*
	N=10	6.35
	N=20	6.63
PID-ZN	N=2	6.93
	N=10	5.99*
	N=20	6.03
PID-CC	N=2	8.23
	N=10	7.17*
	N=20	7.20

### 2.3 Controller Performance index

The performance evaluation was carried out based on transient response characteristics, including per cent overshoot (%OS), rise time (Tr) and settling time (Ts). Besides, three other performance criteria were also included such as Integral Squared Error (ISE), Integral Absolute Error (IAE) and Integral Absolute Time Weighted Error (ITEA). The ISE index provides more weight to smaller error values by squaring them. It is helpful to indicate overshoot after a step change or disturbance as a significant control error is expected when it occurs. ISE integrates the squared error of the system over a period of time given by:

$$ISE = \int_0^{\infty} e^2(t) dt \quad (5)$$

The IAE index penalize all errors regardless the positive and negative sign by integrating its absolute values over a period of time given by:

$$IAE = \int_0^{\infty} |e(t)| dt \quad (6)$$

Meanwhile, ITEA integrates the time multiplied with an absolute error of the system. It helps to emphasize errors that happen late in time, and less weight is placed on errors that occur earlier within the time frame. The ITEA index is given by:

$$ITEA = \int_0^{\infty} t |e(t)| dt \quad (7)$$

### 3. Results and discussion

#### 3.1 Transient response

Figure 4 illustrates the transient response of the system during the step test simulation study. It can be observed that PID-AMIGO exhibit the lowest overshoot value as compared to PID-CC and PID-ZN controllers. Meanwhile, the shortest rise time was achieved using PID-CC, and the PID-ZN controller obtained the shortest settling time. As Table 4 shows, the overshoot percentage for PID-AMIGO controller has improved by 82.8% and 84.8% from PID-ZN and PID-CC controller, respectively. In addition, it is also apparent from this table that there is a significant reduction of ISE, IAE and ITAE indexes for PID-AMIGO controller as compared to PID-ZN and PID-CC.

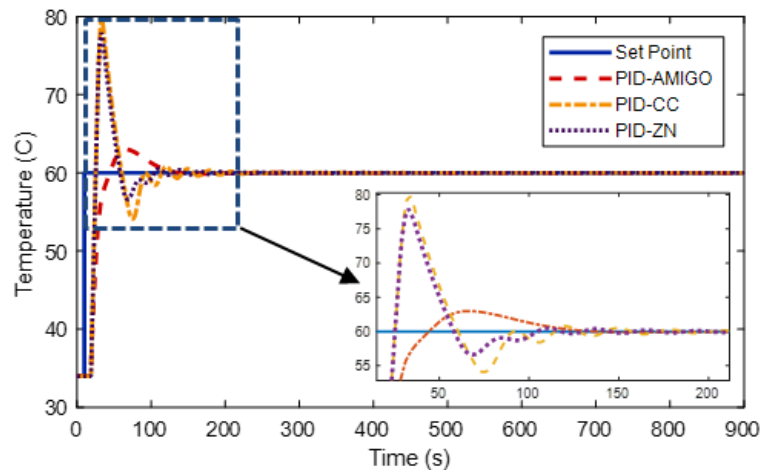


Figure 4. Transient response of the system

Table 4. The performance of each controller during step test

Controller	Rise time (s)	Settling time (s)	ISE	IAE	ITAE
PID-AMIGO	15.06	92.82	*8.809x10 <sup>3</sup>	*5.597x10 <sup>2</sup>	*2.048x10 <sup>4</sup>
PID-ZN	5.08	80.01*	1.141x10 <sup>4</sup>	6.935x10 <sup>2</sup>	2.41x10 <sup>4</sup>
PID-CC	5.024*	131.31	1.294x10 <sup>4</sup>	8.827x10 <sup>2</sup>	3.424x10 <sup>4</sup>

#### 3.2 Load disturbance test

The comparison of the load disturbance rejection feature of the controllers used in this study is shown in Figure 5. A step-change in the load variable was introduced at  $t = 450$  s, causing a sudden transient shift in the process temperature. It is apparent from this figure that the PID-AMIGO controller exhibits the lowest overshoot percentage. All three controllers managed to recover the desired temperature to achieve a steady-state value after a period of time. A close inspection of the figure indicated that the recovery time was measured at 100 s, 107.5 s and 99 s for PID-AMIGO, PID-ZN and PID-CC, respectively. On the other hand, it can be clearly seen in table 5, the resulting ISE ( $1.403 \times 10^4$ ) and IAE ( $9.888 \times 10^2$ ) for AMIGO tuning rules are also much lower than the one obtained using Ziegler-Nichols and Cohen-Coon tuning rules. These findings suggest that the PID-AMIGO controller has better disturbance rejection features.

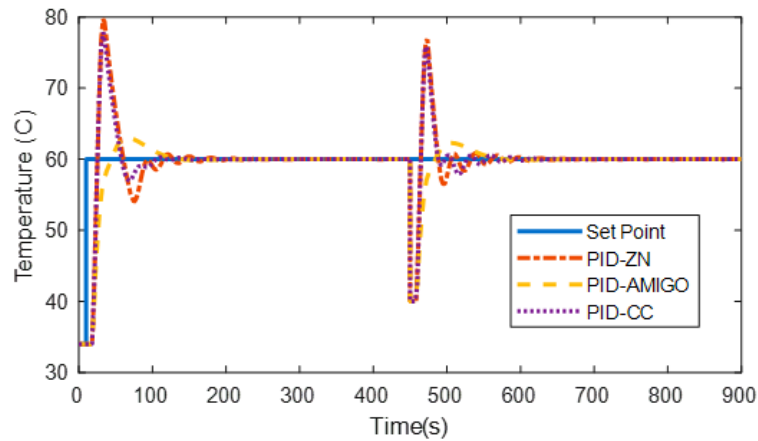


Figure 5. The system responds towards load disturbance

Table 5. The controller performance during load disturbance test

Controller	Recovery time (s)	% OS	ISE	IAE
PID-AMIGO	100 s	3.8	$1.403 \times 10^4$	$9.888 \times 10^2$
PID-ZN	107.5 s	28.07	$1.82 \times 10^4$	$1.194 \times 10^3$
PID-CC	99 s	26.42	$2.022 \times 10^4$	$1.377 \times 10^3$

### 3.3 Set-point tracking

Two input types were used to test the controller’s performance on set-point tracking, consisting of ramp input and step change at  $t=200$  s and  $t = 550$  s. The ramp input is used to indicate a slow, varying set-point, where the step change is used to indicate sudden change in the set point at a specific time point within the process. Figure 6 and 7 indicates the output response of the controllers for a given set-point change. Table 6 compares the ISE and IAE values obtained from the simulation using the controllers under study. As can be seen from the table, the PID-CC controller performed better in handling slow, varying set-point change indicated by the lower value of both ISE and IAE at  $8.615 \times 10^2$  and  $6.426 \times 10^2$  respectively. Meanwhile, PID-AMIGO responded better when given input step change at  $t=200$  s and  $t= 500$  s, indicated by the lowest ISE and IAE values at  $3.485 \times 10^3$  and  $3.485 \times 10^3$  respectively.

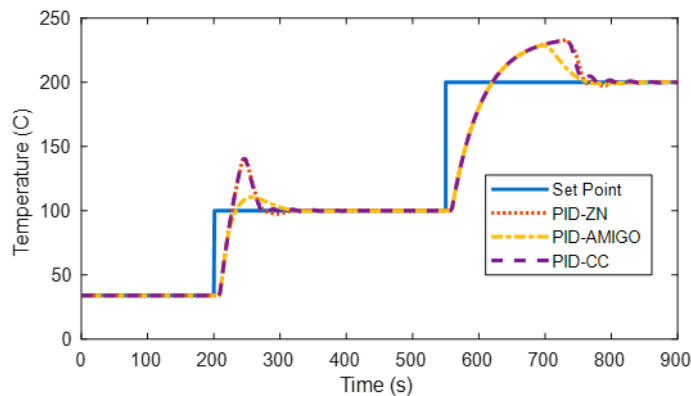


Figure 6. The controller response comparison during set-point tracking test

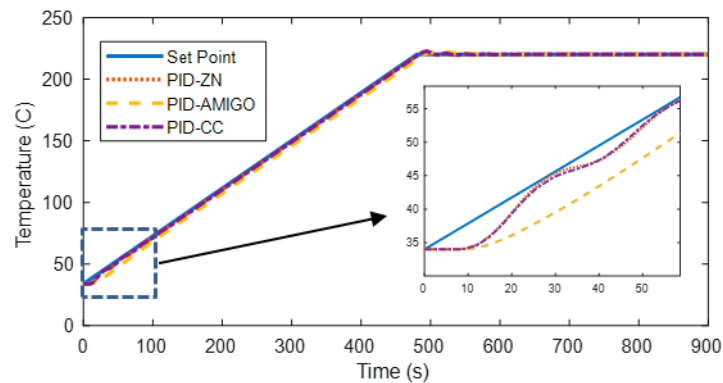


Figure 7. The controller response comparison given a slow varying set-point change.

**Table 6.** Controller performance comparison for set point tracking test

Controller	Input type	ISE	IAE
PID-AMIGO	Ramp	$9.195 \times 10^3$	$2.174 \times 10^3$
	Set point change	$*3.485 \times 10^5$	$*3.485 \times 10^5$
PID-ZN	Ramp	$8.816 \times 10^2$	$6.469 \times 10^2$
	Set point change	$4.03 \times 10^5$	$8.636 \times 10^3$
PID-CC	Ramp	$*8.615 \times 10^2$	$*6.426 \times 10^2$
	Set point change	$3.994 \times 10^5$	$8.568 \times 10^3$

#### 4. Conclusion

This study aimed to assess the PID controller performance in controlling coffee roasting temperature using selected tuning methods. Based on the simulation results, the PID-AMIGO controller offers better transient performance, robustness towards load disturbance and the ability to track different set-point settings at  $t = 200$  s and  $t = 550$  s. However, the PID-CC controller outperforms the PID-AMIGO and PID-ZN controller if a slow, varying set-point input is applied.

#### Acknowledgement

The authors would like to thank all parties involved in this project, including staff members from FKE UiTM Terengganu, UiTM Shah Alam and RMU UiTM Terengganu. We also sincerely acknowledge the efforts done by Sabah's coffee producer, Sabarica Coffee ([www.sabarica.com](http://www.sabarica.com)), for supplying specialty grade fresh coffee beans from local coffee plantations from Sabah, Malaysia.

#### 5. References

- [1] M. Münchow, J. Alstrup, I. Steen, and D. Giacalone, "Roasting Conditions and Coffee Flavor: A Multi-Study Empirical Investigation," *Beverages*, vol. 6, no. 2, p. 29, May 2020, doi: 10.3390/beverages6020029.
- [2] H. Schwartzberg, "Improving industrial measurement of the temperature of roasting coffee beans.," in *21st International Conference on Coffee Science, Montpellier, France, 11-15 September, 2006*, 2007, pp. 606–610.
- [3] F. Sarghini, E. Fasano, A. De Vivo, and M. C. Tricarico, "Influence of roasting process in six coffee Arabica cultivars: Analysis of volatile components profiles," *Chem. Eng. Trans.*, vol. 75, pp. 295–300, 2019.



- [4] K. Ghousiya Begum, A. Seshagiri Rao, and T. K. Radhakrishnan, "Assessment of Proportional Integral Derivative Control Loops for Large Dominant Time Constant Processes," *Chem. Prod. Process Model.*, vol. 15, no. 1, pp. 1–10, 2020, doi: 10.1515/cppm-2019-0024.
- [5] D. I. Wilson, *Advanced Control using MATLAB or Stabilising the unstaibilisable*. David I. Wilson, 2015.
- [6] S. B. Prusty, S. Padhee, U. C. Pati, and K. K. Mahapatra, "Comparative performance analysis of various tuning methods in the design of PID controller," *IET Conf. Publ.*, vol. 2015, no. CP683, pp. 43–48, 2015, doi: 10.1049/cp.2015.1604.
- [7] A. A. Azman, N. N. Mohammad, N. H. Sidek, and M. F. Ali, "FOPDT Modelling and Controller Comparative Study for Smart Tube Aqua Filter ( STAF )."
- [8] M. H. Marzaki, M. H. A. Jalil, H. M. Shariff, R. Adnan, and M. H. F. Rahiman, "Comparative study of Model Predictive Controller (MPC) and PID Controller on regulation temperature for SSISD plant," in *5th IEEE Control and System Graduate Research Colloquium, ICSGRC 2014*, 2014, pp. 136–140.
- [9] N. Yergenson and D. E. Aston, "Monitoring coffee roasting cracks and predicting with in situ near-infrared spectroscopy," *J. Food Process Eng.*, vol. 43, no. 2, pp. 1–10, 2020, doi: 10.1111/jfpe.13305.
- [10] N. Yergenson and D. E. Aston, "Online determination of coffee roast degree toward controlling acidity," *J. Near Infrared Spectrosc.*, vol. 28, no. 4, pp. 175–185, 2020, doi: 10.1177/0967033520924493.
- [11] B. Ripper, C. R. Kaiser, and D. Perrone, "Use of NMR techniques to investigate the changes on the chemical composition of coffee melanoidins," *J. Food Compos. Anal.*, vol. 87, p. 103399, 2020, doi: 10.1016/j.jfca.2019.103399.
- [12] M. T. Miskon, M. H. Fazalul Rahiman, and M. N. Taib, "Modelling of Sabahan Coffee Bean Roasting process using Optimized FOPDT Function," in *2020 IEEE Conference on System, Process and Control (ICSPC)*, 2020, no. December, pp. 11–12.
- [13] D. J. Cooper, *Practical Process Control Using Loop-Pro Software*. Control Station, Inc. Tolland, 2005.
- [14] K. J. Åström, T. Hägglund, and K. J. Astrom, *Advanced PID control*, vol. 461. ISA-The Instrumentation, Systems, and Automation Society Research Triangle, 2006.